

This is an Open Access document downloaded from ORCA, Cardiff University's institutional repository: <https://orca.cardiff.ac.uk/id/eprint/129413/>

This is the author's version of a work that was submitted to / accepted for publication.

Citation for final published version:

Moore, Andy, Yudovskaya, Marina, Proyer, Alexander and Blenkinsop, Thomas 2020. Evidence for olivine deformation in kimberlites and other mantle-derived magmas during crustal emplacement. *Contributions to Mineralogy and Petrology* 175 (2) , 15. [10.1007/s00410-020-1653-8](https://doi.org/10.1007/s00410-020-1653-8)

Publishers page: <http://dx.doi.org/10.1007/s00410-020-1653-8>

Please note:

Changes made as a result of publishing processes such as copy-editing, formatting and page numbers may not be reflected in this version. For the definitive version of this publication, please refer to the published source. You are advised to consult the publisher's version if you wish to cite this paper.

This version is being made available in accordance with publisher policies. See <http://orca.cf.ac.uk/policies.html> for usage policies. Copyright and moral rights for publications made available in ORCA are retained by the copyright holders.



[lick here to view linked References](#)

1 **EVIDENCE FOR OLIVINE DEFORMATION IN KIMBERLITES AND OTHER MANTLE-DERIVED MAGMAS**  
2 **DURING CRUSTAL EMPLACEMENT**

3 Version: Revised

4  
5 Andy Moore<sup>1\*</sup>, Marina Yudovskaya<sup>2,3</sup>, Alexander Proyer<sup>4</sup> Thomas Blenkinsop<sup>5</sup>

6  
7 <sup>1</sup>Dept. of Geology, Rhodes University, Artillery Road, Grahamstown, South Africa.

8  
9 <sup>2</sup>Institute of Geology of Ore Deposits, Petrography, Mineralogy and Geochemistry, RAS, 35  
10 <sup>7</sup> Staromonetny, Moscow 119017, Russia

11  
12 <sup>8</sup> <sup>3</sup>EGRI, University of the Witwatersrand, Private Bag 3, Wits 2050, South Africa

13  
14 <sup>9</sup> <sup>4</sup>Botswana International University of Science and Technology, Private Bag 16, Palapye, Botswana.

15  
16 <sup>10</sup> <sup>5</sup>School of Earth and Ocean Sciences, Cardiff University, Cardiff, Wales, U.K. CF10 3XQ

17  
18 <sup>11</sup>  
19  
20 <sup>12</sup> [\\*andy.moore.bots@gmail.com](mailto:andy.moore.bots@gmail.com) (Corresponding author).

21  
22 <sup>13</sup>  
23  
24  
25 **14 Abstract**

26  
27 <sup>15</sup> This paper highlights published and new field and petrographic observations for late-stage  
(crustal

28 <sup>16</sup> level) deformation associated with the emplacement of kimberlites and other mantle-derived <sup>29</sup>  
30 <sup>17</sup> magmas. Thus, radial and tangential joint sets in the competent 183 Ma Karoo basalt wall rocks to  
31  
32 <sup>18</sup> the 5 ha. Lemphane kimberlite blow in northern Lesotho have been ascribed to stresses linked to  
33

1  
2  
3  
4  
5  
6  
7  
8  
9  
34  
35  
36  
37  
38  
39  
40  
41  
42  
43  
44  
45  
46  
47  
48  
49  
50  
51  
52  
53  
54  
55  
56  
57  
58  
59  
60  
61  
62  
63  
64  
65

19 eruption of the kimberlite magma. Further examples of emplacement-related stresses in  
20 kimberlites are brittle fractures and close-spaced parallel shears which disrupt olivine macrocrysts.  
21 In each of these examples, there is no evidence of post-kimberlite regional tectonism which might  
22 explain these features, indicating that they reflect auto-deformation in the kimberlite during or  
23 immediately post-emplacement. On a microscopic scale, these inferred late-stage stresses are  
24 reflected by fractures and domains of undulose extinction which traverse core and margins of some  
25 euhedral and anhedral olivines in kimberlites and olivine melilitites. Undulose extinction and kink  
26 bands have also been documented in olivines in cumulates from layered igneous intrusions. Our  
27 observations thus indicate that these deformation features can form at shallow levels (crustal  
28 pressures), which is supported by experimental evidence. Undulose extinction and kink bands have  
29 previously been presented as conclusive evidence for a mantle provenance of the olivines – i.e. that  
30 they are xenocrysts. The observation that these deformation textures can form in both mantle and  
31 crustal environments implies that they do not provide reliable constraints on the provenance of the  
32 olivines. An understanding of the processes responsible for crustal deformation of kimberlites  
could 33 potentially refine our understanding of kimberlite emplacement processes.

## 35 Introduction

36  
37 Olivine is always the dominant phase in kimberlites, comprising an average of 50% of the total rock  
38 volume (Skinner, 1989). Skinner divided kimberlitic olivines on the basis of size into small, often

1  
2  
3  
4  
5  
6  
7  
8  
9  
10 39 euhedral micro-phenocrysts and phenocrysts, <0.5mm in length, and larger (>0.5mm), often  
11  
12 40 anhedral and rounded macrocrysts, often considered to be xenocrysts. Scott-Smith et al (2013)  
13 41 subsequently suggested that the term macrocryst be restricted to olivines > 1.0 mm, but noted that 14  
15 42 it should be used with a non-genetic connotation. It should be stressed, however, that these sub-  
16  
17 43 divisions are artificial constraints, as kimberlitic olivines typically show a size continuum rather than  
18  
19 44 a bimodal distribution (Moore, 1988; Moss et al., 2010).  
20  
21 45  
22  
23  
24 46 There are strongly divergent views on the origin of kimberlitic olivines. Several recent publications  
25 47 have concluded that the cores of all kimberlitic olivines are xenocrysts, derived from disaggregated  
26  
27 48 mantle peridotites, and that only the outer rims crystallized from the host magma (e.g. Kamenetsky 28  
29 49 et al, 2008; Brett et al., 2009; Arndt et al., 2010; Lim et al., 2018). In contrast, Moore (1988; 2012;  
30  
31 50 2017) argued that the majority of kimberlitic olivines are cognate phenocrysts. Skinner (1989) took  
32  
33 51 an intermediate view, concluding that the euhedral olivine phenocrysts and microphenocrysts are  
34 52 cognate to the kimberlite, but that the majority of macrocrysts are xenocrysts.  
35  
36  
37 53  
38  
39 54 These contrasting interpretations have important implications for the composition and generation of 40  
41 55 kimberlite magmas. If a majority of olivines are cognate, this would point to a highly Mg-rich  
42  
43 56 primitive kimberlitic liquid, whereas the xenocrystal model implies a carbonatitic, relatively Mg-poor  
44  
45 57 primary magma. It is therefore clearly critical to determine the origin of kimberlite olivines in order

1  
2  
3  
4  
5  
6  
7  
8  
9  
46  
47  
48  
49  
50  
51  
52  
53  
54  
62  
63  
64  
65  
66  
67  
68  
10  
11  
12  
13  
14  
15  
16  
17  
18  
19  
20  
21  
55  
56  
57  
58  
59  
60  
61  
62  
63  
64  
65

58 to understand the processes responsible for producing kimberlite magmas.

59  
60 Various criteria have been proposed to distinguish between a xenocrystal or cognate origin for  
61 kimberlitic olivines. Thus, several authors (e.g. Arndt et al., 2010; Bussweiler et al., 2015) note that  
62 compositions of the most refractory olivines in kimberlites overlap the range typical of mantle  
63 peridotite xenoliths. However, this does not preclude a cognate origin, as the first olivine to  
64 crystallize from a magma generated in equilibrium with mantle olivines would be expected to be  
65 closely similar in composition to those in the mantle source. Subsequent crystallization would result  
66 in decreasing Mg# of the liquidus olivine, but would result in limited initial change in Ni content, as  
67 decreasing Mg concentration in the magma would be accompanied by an increase in the Ni partition  
68 coefficient (Hart and Davis, 1978; Moore, 2017). The consequence is that olivines produced by  
fractional crystallization of a magma could, at least in principle, overlap the range of Mg # and Ni  
concentrations typical of mantle peridotites.

71  
72 Sharp compositional gradients that are typical of rims of kimberlitic olivines have also been used to  
73 argue that the olivine cores are mantle-derived xenocrysts (Bussweiler et al., 2015). However,  
74 kimberlites experience complex late-stage P-T-X paths, with rapidly decreasing temperature  
75 associated with initiation of fluidization of the magma. Rapidly decreasing temperature would, in  
76 turn, result in a sharp increase in  $K_{Ni}$  (olivine-liquid) (Matzen et al., 2013), which could account for  
77 the steep decrease in Ni which is characteristic of olivine rims (Moore, 2017).

1  
2  
3  
4  
5  
6  
7  
8  
9  
22

23 78

24  
25

26 79 Some (though not all) olivines in mantle peridotites are characterized by internal deformation

27

28 80 features, including undulose extinction, kink banding and mosaic recrystallization, which have  
been

29 81 ascribed to dynamic stresses in the mantle. Such deformation textures have accordingly been 30

31 82 considered to be diagnostic criteria for recognizing mantle-derived olivine xenocrysts (e.g. Skinner,

32

33 83 1989; Scott-Smith et al., 1989; Cordier et al. 2017). Brett et al. (2015) have reported that fractures

34

35 84 traversing some olivines terminate at the marginal rind, which they infer to be reflect a late,

36

37 85 magmatic overgrowth to a mantle-derived xenocryst.

38

39 86

40

41

42 87 The purpose of this paper is to highlight published and new field and petrographic observations for

43 88 late-stage (crustal level) deformation associated with the emplacement of kimberlites. Evidence is 44

45 89 presented to demonstrate that olivine deformation textures, which have previously been used to

46

47 90 argue for a mantle provenance, can also form in kimberlites and some other mantle-derived

48

49 91 magmas in response to stresses associated with emplacement and solidification at crustal depths.

50

51 92

52

53

54 93 It should be stressed, at the outset, that we are not disputing the existence of olivine xenocrysts in

94 general or a mantle origin for some olivine deformation textures. Rather, if similar textures can

55

56

57

58

59

60

61

62

63

64

65

1  
2  
3  
4  
5  
6  
7  
8  
9

95 form at shallow (crustal) depths, they do not, on their own, provide reliable evidence for  
96 distinguishing whether the olivines have a mantle provenance – i.e. are xenocrysts – or are cognate  
97 phenocrysts.

98

99 **Field evidence for deformation associated with crustal kimberlite** 100  
101 **emplacement**

10  
11

12 **101 Previous studies**

13

14 **102**

15

16

17 **103** A study of the Lemphane kimberlite dykes and blows in the northern Lesotho highlands (Kreston,

18

19 **104** 1973) highlighted exceptionally important, and perhaps overlooked evidence of late-stage (crustal)

20

**105** deformation affecting kimberlite wall rocks. Kreston measured joints in the rigid Karoo basalt wall

21

**106** rocks to the 5.7 ha Lemphane kimberlite blow, and showed that they defined sets that were both

22

**107** tangential (Fig. 1) and radial to the kimberlite margin. The width of the wall rocks affected by these

23

**108** joint sets was not specified, but Kreston observed that they did not persist over any appreciable

24

**109** distance from the Lemphane blow, and were absent in the basalts 25m from the kimberlite contact.

25

**110** As the Karoo basalts of the Lesotho highlands, dated at ~183 Ma. (Marsh et al., 1997), do not show

26

**111** evidence of regional tectonic deformation, Kreston (1973) concluded that the joint sets marginal to

27

**112** the Lemphane blow were linked to stresses that “are obviously caused by the kimberlite”.

28

29

30

31

32

33

34

35

36

37

38

39

40

41

42

1  
2  
3  
4  
5  
6  
7  
8  
9  
35  
36  
37  
38  
39  
40  
41  
42  
44  
45  
46  
47  
48  
49  
50  
51  
53  
54  
  
124  
  
125  
126  
  
127  
128  
129  
  
10  
11  
12  
13  
  
55  
56  
57  
58  
59  
60  
61  
62  
63  
64  
65

113

114

Kreston and Dempster (1973) documented a hardebank kimberlite dominated by olivine crystals,

115

with very minor amounts of interstitial serpentine and perovskite, from the Malibamatso dyke

116

swarm (northern Lesotho highlands) (Fig. 2). The kimberlite is traversed by parallel incipient shear

117

zones, and these authors noted that there is a tendency for some of the olivines to show “cleavages” 43

118

parallel to these lineaments. However, they did not present evidence to show that these partings

119

were crystallographically controlled, and they may be fractures. In view of the absence of evidence

120

for regional deformation post-dating eruption of the Karoo basalt wall rocks, Kreston and Dempster

121

(1973) concluded that both the incipient shears and the cleavages (or fractures) in the olivines

122

developed during the later stages of intrusion of the kimberlite dyke – in other words at crustal 52

123

levels.

124

### 125 **Supporting observations**

126

127

Figs 3a & 3b illustrate a hand specimen from a kimberlite dyke associated with the Cambrian age

128

(~530 Ma) economic 3 ha Murowa kimberlite pipe, located to the southwest of Masvingo in south-

129

central Zimbabwe (Smith et al., 2004). A majority of olivine macrocrysts in this specimen are 130

characterized by pronounced closely spaced fractures with a sub-parallel alignment, with some

10 131

showing a second parting set with an oblique orientation.



1  
2  
3  
4  
5  
6  
7  
8  
9  
14  
15  
16  
17  
18  
19  
20  
21  
22  
23  
24  
25  
26  
27  
28  
29  
30  
31  
32  
33  
34  
35  
36  
37  
38  
39  
40  
41  
42  
43  
44  
55  
56  
57  
58  
59  
60  
61  
62  
63  
64  
65

133 Micro-faults associated with slickenslides and development of chlorite on the fault plane, were

134 observed in a number of core sections, drilled from surface into the BK16 kimberlite of the Orapa

135 cluster. Fig. 3c illustrates one of these micro-faults. The wall rocks are ~183 Ma Karoo basalts,

136 which do not appear to have been affected by post-eruption deformation.

138 Fig. 3d illustrates a section of core (hole DTP 12N, 78.3m) from the mid-Cretaceous du Toitspan

139 kimberlite (Kimberley cluster, South Africa), which is traversed by calcite-filled brittle fractures,

some

140 of which have disrupted olivine macrocrysts.

142 **Microscopic evidence for late-stage deformation of olivines in kimberlites, 36 143**  
143 **olivine melilitites and layered intrusions**

144 **Kimberlites**

145 Deformation textures in kimberlitic olivine, when present, are more common in the larger,  
anhedral

1  
2  
3  
4  
5  
6  
7  
8  
9  
45  
46  
47  
48  
49  
50  
51  
52  
53  
54  
10  
11  
12  
13  
14  
15  
16  
17  
18  
19  
20  
21  
55  
56  
57  
58  
59  
60  
61  
62  
63  
64  
65

147 olivines (Skinner, 1989). However, Moore (1988) reported undulose extinction in small euhedral  
148 olivines in some kimberlites. This is illustrated by the euhedral olivine from the De Beers kimberlite  
149 (Kimberley cluster) in Fig. 4 a & b. The grain exhibits non-uniform extinction domains, some of  
150 which extend to the edge of the olivine. Skinner (1989) expressed the view that undulose  
extinction

151 in euhedral kimberlite olivines is very uncommon, but further in-depth investigation is required to  
152 confirm this generalization.

153  
154 Note that fluid inclusions are present both within the core and margin of the crystal illustrated in Fig.  
155 4a&b, and that fractures traversing the mineral extend to the margins. In Fig. 4c, the core and rim of  
156 the largest olivine (top centre) are distinguished by light and dark grey interference colours  
157 respectively. Some of the fractures in this olivine also traverse both core and rim. Several of the  
158 smaller olivines are also characterized by fractures traversing the whole crystal (e.g. the  
olivine in  
159 the lower right of this image).

160  
161 The proportions of olivines displaying undulose extinction and other deformation textures seem to  
162 vary considerably between kimberlites, but such differences have not been systematically  
163 quantified. Thus, Scott-Smith et al (1989) noted that in the Kapamba lamproites (Luangwa Valley,  
164 Zambia), undulose extinction was common in both the large anhedral and small euhedral olivines.  
165 They observed that this made it difficult to distinguish cognate phenocrysts from exotic xenocrysts.

1  
2  
3  
4  
5  
6  
7  
8  
9  
22  
23  
24  
26  
27  
28  
29  
30  
31  
32  
33  
34  
35  
36  
37  
38  
39  
40  
41  
42  
43  
45  
46  
47  
48  
49  
50  
52  
53  
54  
55  
56  
57  
58  
59  
60  
61  
62  
63  
64  
65

166 In contrast, undulose extinction in olivines, including macrocrysts, is absent, subdued or rare in some

167 kimberlites. Examples of kimberlites dominated by relatively undeformed macrocrysts are 25  
168 illustrated by Mitchell (1997) for the Kimberley cluster (Plates 74, 76, 78 & 80); Pipe 200, Lesotho  
169 (Plate 84); Vtorogodnitsa, Russia (Plate 86); Lac de Gras, Canada (Plate 90) and Somerset Island,  
170 Canada (Plates 94 & 96). However, virtually all of the olivines shown in the flagged images from  
171 Mitchell (1997) are characterized by fractures which traverse grain interiors and rims.

172  
173 **Olivine melilitites**

174  
175 Olivine is the dominant phenocryst phase in olivine melilitites from the Namaqualand-Bushmanland  
176 area of north-western South Africa. Some crystals are euhedral, with bipyramid terminations and a 44  
177 roughly 2:1 aspect ratio (Fig. 4d). However, many are characterized by re-entrants typical of hopper  
178 olivines (Moore and Erlank, 1979), comparable to the magmatic growth forms observed in  
179 experimental studies involving a small degree of under-cooling (Donaldson, 1976; Faure et al.,  
2003)

180 An example of a “hopper” olivine phenocryst, from the Dikdoorn pipe (Namaqualand) is illustrated in 51  
181 Fig. 4e (PPL) and 4f (XPL).

182

1  
2  
3  
4  
5  
6  
7  
8  
9

183 Figure 5 (data from Moore and Erlank, 1979) illustrates a representative pattern of olivine  
184 compositional variation from an olivine melilitite sample from a pipe on the farm Biesiesfontein, in  
185 the Namaqualand cluster (Moore & Erlank, 1979). A majority of the olivine cores define a trend of  
186 decreasing Mg#, with a relatively small decrease in Ni, and normal outward zonation from the core,  
187 except at the very edges, which define a trend of marked reverse zonation. A very subordinate 188  
group of olivines with relatively Fe-rich olivine cores are characterized by inverse zonation.

189

10 190 The zonation trend shown by the majority of olivine cores was interpreted by Moore and Erlank  
11 (1979) to reflect Raleigh-type crystallization of olivine phenocrysts from the melilitite parental liquid.

12 191  
13  
14 192 The reverse zoning defined by the rims was ascribed to late-stage co-precipitation with Fe-oxides,  
15  
16 193 present as intergrowths at the olivine margins. The rare olivines showing inverse zoning are  
probably

17 194 related to the Cr-poor megacryst suite (Moore and Costin, 2016).  
18  
19

20 195  
21

## 22 196 **Layered igneous complexes**

23  
24

25 197  
26

27 198 Olivines with undulose extinction, kink bands and occasionally granular textures, reflecting  
28  
29 199 recrystallization, have been reported from cumulates from the Lower Zone of the Northern Limb of  
30  
31 200 the Bushveld Igneous Complex (BIC) (Yudovskaya et al, 2013). Examples, taken from this study are  
32

55  
56  
57  
58  
59  
60  
61  
62  
63  
64  
65

1  
2  
3  
4  
5  
6  
7  
8  
9  
33  
34  
35  
36  
37  
38  
39  
40  
41  
42  
43  
44  
45  
46  
47  
48  
49  
50  
51  
52  
53  
54  
  
212  
213  
214  
215  
216  
  
219  
  
55  
56  
57  
58  
59  
60  
61  
62  
63  
64  
65

illustrated in Figs. 6g & h. In sample UMT6-1449 (Fig. 6g), the majority of the olivines show undulose extinction. They are characterized by a very restricted compositional range (Mg # 89.85 – 90.02; Ni = 0.147 – 0.152, n = 5; (Yudovskaya et al., 2013). Fig. 6h illustrates kink bands in olivines from a harzburgite cumulate, Zone of the northern limb of the BIC.

Kink-banded olivines have also been described in other crustal complexes such as the Great Dyke (Wilson, 1982), the Poyi ultramafic intrusion (Yao et al., 2017) and Duke Island complex (Li et al., 2012). Yudovskaya et al. (2018) have also reported phlogopite, clinopyroxene, chromite and plagioclase with deformation textures from the northern limb of the BIC.

**Discussion**

The Lesotho Karoo basalts, dated at ~183 Ma (Marsh et al., 1997), do not show evidence of regional tectonic deformation. Kreston (1973) therefore concluded that the tangential (Fig. 1) and radial joint sets associated with the Lemphane blow are “obviously” caused by emplacement of the kimberlite. The same argument was used by Kreston and Dempster (1973) to conclude that the incipient shears and cleavages (or fractures) in olivines in the Malibamatso dyke must have been developed during the late stages of emplacement of the kimberlite magma – in other words, at crustal levels.

1  
2  
3  
4  
5  
6  
7  
8  
9  
10  
11  
12  
13  
14  
15  
16  
17  
18  
19  
20  
21  
22  
23  
24  
25  
26  
27  
28  
29  
30  
31  
32  
33  
34  
35  
36  
37  
38  
39  
40  
41  
42  
55  
56  
57  
58  
59  
60  
61  
62  
63  
64  
65

220 Similar considerations are relevant to account for the close-spaced joint sets traversing the  
221 kimberlitic olivines in the Murowa kimberlite dyke, illustrated in Fig. 3 a&b. There is no evidence of  
222 regional penetrative deformation of this portion of the Zimbabwe craton subsequent to kimberlite  
223 emplacement. It further seems most unlikely that this strong preferred orientation of the olivine  
224 joint sets is mantle-derived, as disaggregation of sheared olivines from a mantle xenolith during  
225 turbulent transport to the surface would produce a non-systematic orientation pattern. These  
226 observations thus provide evidence that development of the close-spaced fracture sets was a  
227 response to late-stage stresses within the near solidified kimberlite magma – in other words at  
228 crustal levels. Similarly, the absence of post-eruption deformation in the ~183 Ma Karoo basalts  
229 forming the wall-rocks to the BK-16 kimberlite in the Orapa cluster (Botswana) indicates that the  
230 micro-faults illustrated in Fig. 3c reflect late-stage deformation related to stresses associated with  
231 emplacement and cooling of the kimberlite.

232

233 The fractures in the Du Toitspan kimberlite , which may disrupt olivine macrocrysts (Fig. 3d), provide  
234 evidence for solid state, syn- to post-emplacement deformation of kimberlites, thus precluding  
235 their  
236 formation as decompression fractures formed within the mantle, such as those reported in some  
237 olivines by Brett et al. (2015). The absence of deformation events in the cratonic host country rocks  
suggests that the latest possible timing of the (auto-)deformation within the kimberlite was

1  
2  
3  
4  
5  
6  
7  
8  
9  
43  
44  
45  
46  
47  
48  
49  
50  
51  
52  
54  
244  
245  
246  
247  
  
248  
and  
  
249  
250  
251  
10 252  
  
11  
12  
13  
14  
15  
16  
18  
19  
  
55  
56  
57  
58  
59  
60  
61  
62  
63  
64  
65

238 immediately post-emplacment.

239

240 Collectively, the field evidence documented show that emplacement of kimberlites is associated

241 with internal stresses that exist over the period of cooling and consolidation of the magma. These

242

242 stresses must have been of sufficient magnitude to impose the radial and tangential fracture sets on

243 the rigid basalt wall rocks to the Lemphane kimberlite blow, documented by Kreston (1973).

244 Incipient shearing of kimberlites (Fig. 2), development of closely-spaced fracture sets (Fig. 3a&b),

245 minor faults with slickensides (Fig. 3c) and brittle fractures (Fig 3d) are interpreted to reflect a range

246 of responses to internal stresses during and immediately following kimberlite emplacement.

247

248 The evidence presented also demonstrates that some kimberlitic olivines experienced fracturing  
and

249 deformation subsequent to the development of the euhedral crystal margins, and thus during the

250 late stages of kimberlite emplacement (Figs 2 & 3; 4a-c). Thus, undulose extinction and fractures

251 extending from the core to the margin of the euhedral olivine from the de Beers kimberlite (Fig. 4

10 252 a&b) point to deformation during the late stages of emplacement and crystallization of the

11 253 kimberlite magma.

14 254

16 255 Moore and Erlank (1979) concluded from the study of olivines in the Namaqualand olivine melilitites 17

18 256 that the presence of hopper growth forms, indicative of magmatic crystallization, coupled with the

1  
2  
3  
4  
5  
6  
7  
8  
9  
20  
21  
22  
23  
24  
25  
26  
27  
28  
29  
30  
31  
32  
33  
34  
35  
36  
37  
38  
39  
40  
41  
42  
43  
44  
45  
46  
47  
48  
49  
50  
51  
55  
56  
57  
58  
59  
60  
61  
62  
63  
64  
65

257 zonation pattern defined by the majority of cores, which is compatible with Raleigh-type  
258 crystallization, indicate that the overwhelming majority of olivines in the Namaqualand melilitites  
259 have a magmatic origin – i.e. are cognate phenocrysts and not xenocrysts. This interpretation is  
260 supported by the absence of olivines with compositions typical of mantle peridotites (Mg # > 89)  
261 (Fig. 5). The euhedral olivine from the WAT pipe (Namaqualand Cluster) is characterized by  
262 domains of contrasting extinction traversing core and rim of this crystal (Fig. 4d). Similarly, the  
263 hopper olivine crystal illustrated in Fig. 4 e & f is characterized by undulose extinction and  
fractures,  
264 both extending from the interior to the margin. The deformation textures illustrated in Figs. 4d-f  
265 must therefore reflect post-crystallization deformation at crustal levels.  
266  
267 Collectively, the evidence presented demonstrates that at least some olivines in kimberlites, olivine  
268 melilitites and layered complexes have experienced post-crystallization stresses at crustal pressures  
269 and temperatures, which have produced strain features similar to those which characterize olivine  
in  
270 some mantle peridotite xenoliths. Thus, we argue that while strain features in olivines, such as  
271 undulose extinction, *may* be inherited from a mantle source, they do not provide unambiguous  
272 evidence for a mantle provenance. This view is in line with conclusions previously drawn by  
273 Yudovskaya et al. (2013) and Yao et al. (2017).



1  
2  
3  
4  
5  
6  
7  
8  
9  
52  
53  
54  
10  
11  
13  
14  
15  
16  
17  
18  
20  
22  
23  
24  
25  
26  
27  
29  
55  
56  
57  
58  
59  
60  
61  
62  
63  
64  
65

274

275 Understanding the detailed origin of the various crustal stress features which we have identified  
in 276 kimberlites and their wall rocks could potentially provide further insights to the later stages of  
277 kimberlite eruption and emplacement. While this is beyond the scope of our primarily  
descriptive 278 study, we suggest a number of potential processes which should be considered:

279

280 A. Kimberlitic wall-rock breccias provide compelling evidence for high energy explosive  
activity  
281 linked to emplacement (Barnett et al., 2011), while Sparks et al. (2006) suggest that  
282 kimberlite eruptions may have been Plinian in character. Deformation textures may be  
283 linked to stresses transmitted through the magma related to explosive eruption. The radial  
284 and concentric structures reported by Kreston may be the result of explosive overpressure  
285 and post-explosive underpressure on the pipe walls, as proposed by Nicolaysen and  
286 Ferguson (1990). Explosive kimberlite eruption offers a potential explanation for the  
287 observation that both small euhedral olivines and large macrocrysts show deformation  
288 textures in the Kapamba lamproites (Scott-Smith et al., 1989). However, this may not  
289 necessarily always be the case, as olivines with different crystallographic orientations may  
290 respond differently to the shock stresses. Also, in individual large macrocrysts, the domains  
291 of undulose extinction often have relatively large areas, greater than those of smaller  
292 euhedral olivine crystals. This might, in part, account for the rarity of deformation features  
293 in smaller olivines.

294 B. Kreston (1973) suggested that internal kimberlite stresses might be linked to post-explosive  
295 torsional forces linked to emplacement of the kimberlite in a plastic or near-solid state.

1  
2  
3  
4  
5  
6  
7  
8  
9  
30  
31  
32  
33  
34  
36  
38  
39  
40  
41  
42  
43  
44  
45  
46  
47  
48  
49  
50  
51  
52  
53  
54  
55  
56  
57  
58  
59  
60  
61  
62  
63  
64  
65

C. Differential stresses in largely solidified magmas may result from chemical reactions, e.g. a partial serpentinization or carbonation.

D. Stresses may be linked to pressure exerted on solidified kimberlite by the magma from a later pulse of eruption. In general, dynamic conditions in a magmatic plumbing system should result in deformation and brecciation.

Kimberlite deformation linked to one or more of the suggested stresses provides a potential explanation for crustal deformation of olivines. It is noted in this regard that experimental evidence demonstrates that undulose extinction and kink bands can develop in olivines down to very low °C), depending on the pressure applied. (Druiventak, et al., 2011). Further, temperatures (20 – 600

low-Ca olivine tends to be more readily deformed, as high Ca contents in olivine creates the called “solute drag” effect, preventing deformations (Yao et al., 2017). The high Ca-contents of kimberlitic micro-phenocryst olivines, and olivine rims would therefore be expected to inhibit plastic deformation.

In addition to the possible mechanisms discussed above, Welsch et al. (2012) have demonstrated that undulose extinction can result directly from crystal growth processes during magmatic crystallization. These authors present evidence that olivine phenocrysts in lava flows associated with the Piton de la Fournaise volcano on Reunion island are composite crystals, formed by parallel dendritic growth with smaller sub-units coalescing to form macrocrysts. However, branch

1  
2  
3  
4  
5  
6  
7  
8  
9  
10  
11  
12  
14  
15  
16  
17  
18  
19  
20  
21  
22  
23  
24  
25  
26  
27  
28  
29  
30  
31  
32  
33  
34  
35  
36  
37  
38  
39  
40  
41  
42  
55  
56  
57  
58  
59  
60  
61  
62  
63  
64  
65

316 misorientations and lattice mismatches can sometimes produce sub-grain boundaries, dislocation  
317 lamellae and undulose extinction, which they noted have formerly been interpreted in terms of  
318 plastic intracrystalline deformation. The undulose extinction in the hopper olivine from the 13  
319 Namaqualand olivine melilitite illustrated in Fig. 3e&f closely matches some of the growth textures  
320 documented by Welsch et al. (2012).  
321  
322 Subsolidus deformation in layered igneous complexes may reflect solid state reactions accompanied  
323 by increase in volume. This may be linked to exsolution and the formation of sympectites that occur  
324 in olivine and pyroxenes. The origin of the exsolutions is controversial (Fleet et al., 1980; Khisina et  
325 al., 2013), and their link with deformation is not resolved. Nevertheless, a sub-solidus origin of  
326 exsolutions, which are particularly common in grains exhibiting kink bands and undulose extinction,  
327 is generally accepted (Yudovskaya et al., 2013, 2018, Yao et al., 2017).

328  
329 **Conclusions**

330  
331 Field and petrographic evidence demonstrate that kimberlites experience a range of stresses during  
332 crustal emplacement, extending to early post-solidification of the magma. The processes

1  
2  
3  
4  
5  
6  
7  
8  
9  
43  
45  
46  
47  
48  
49  
50  
51  
52  
53  
54  
339  
340  
341  
342  
343  
344  
345  
10  
11  
12  
13  
14  
16  
18  
19  
20  
21  
22  
55  
56  
57  
58  
59  
60  
61  
62  
63  
64  
65

333 responsible for these stresses remain speculative, and an understanding of their origin could 44  
334 potentially refine models for kimberlite emplacement. However, irrespective of their origin, such  
335 stresses, possibly coupled with direct crystallization processes, such as those reported by Welsch et  
336 al. (2012), provide a potential explanation for late-stage deformation features such as undulose  
337 extinction, kink banding and fracturing which we have documented in some olivines.

338  
339 We stress, once again, that we do not dispute the existence of olivine xenocrysts in general, or a  
340 mantle origin for some olivine deformation textures. Nevertheless, our study demonstrates that  
341 deformation textures in olivine cannot be used as a reliable indicator of a mantle provenience – i.e.  
342 that olivines showing these deformation textures are invariably xenocrysts.

343  
344 **Acknowledgements**

345 Peter Kreston is thanked for permission to publish the images presented in Figs. 1 & 2, and Dr.  
346 Frieder Reichardt for providing the Murowa dyke sample illustrated in Fig. 3a&b. The core sample  
347 illustrated in Fig. 3d was kindly provided by Petra Diamonds Ltd. Tsodilo Resources (a  
Canadian-  
348 listed diamond exploration company), kindly facilitated a field visit to the company's BK16 15  
349 kimberlite, located in the mid-Cretaceous (~90 Ma) Orapa pipe cluster in central Botswana. Susan 17  
350 Abraham is thanked for help in producing the diagrams.

1  
2  
3  
4  
5  
6  
7  
8  
9  
23 **352**  
24  
25  
26 **353**  
27  
28 **354**  
29  
30 **355**  
31  
32  
33 **356**  
34  
35 **357**  
36  
37  
38 **358**  
39  
40 **359**  
41  
42  
43 **360**  
44  
45 **361**  
46  
47  
48 **362**  
49  
50 **363**  
51  
52  
53 **364**  
54  
    **365**  
  
    **366**  
  
55  
56  
57  
58  
59  
60  
61  
62  
63  
64  
65

1  
2  
3  
4  
5  
6  
7  
8  
9

367

368 **References**

369

370 Arndt NT, Guitreau M, Boullier A-M, Le Roex A, Tomassi A, Cordier P, Sobolev A (2010) Olivine and  
371 the origin of kimberlite. *J Petrol* 51: 573-602

372 Barnett WP, Kurszlauskis S, Tait M, Dirks P (2011) Kimberlite wall-rock fragmentation processes:

10 373 Venetia K08 pipe development. *Bull Volcanol* 73: 941-958

11

12 374 Brett RC, Russell, JK, Andrews GDM, Jones TJ (2015) The ascent of kimberlites: insights from olivine.

13

14 375 *Earth Planet Sci Let* 424: 119-131

15

16 376 Brett RC, Russell JK, Moss S (2009) Origin of olivine in kimberlite: phenocryst or imposter. *Lithos*

17

18 377 *112S*: 201-212

19

20

21 378 Bussweiler Y, Foley SF, Prelević D, Jacob DE (2015) The olivine macrocryst problem: new insights

22 379 from minor and trace element compositions of olivine from the Lac de Gras kimberlites, Canada.

23

24 380 *Lithos* 220-223: 238-252

25

26

27 381 Cordier C, Sauzeat , Arndt NT, Boullier A-M, Batanova V, Barou F (2017) Quantitative modelling of  
the

28 382 apparent decoupling of Mg# and Ni in kimberlitic olivine margins: a reply to the comment on Cordier 29

30 383 *et al.* (2015) by A. Moore. *J Petrol* 58: 391-393

31

32

33 384 Donaldson CH (1976) An experimental investigation of olivine morphology. *Contrib Mineral Petrol*

55

56

57

58

59

60

61

62

63

64

65

1  
2  
3  
4  
5  
6  
7  
8  
9  
34  
35  
36  
37  
38  
39  
40  
41  
42  
43  
44  
45  
46  
47  
48  
49  
50  
51  
52  
53  
54  
396  
397  
399  
400  
401  
402  
403  
10 404  
55  
56  
57  
58  
59  
60  
61  
62  
63  
64  
65

385 57: 187-213

386 Druiventak A, Trepmann CA, Renner J, Hanke K (2011). Low-temperature plasticity of olivine during  
387 high stress deformation of peridotite at lithospheric conditions – an experimental study. Earth  
388 Planet Sci Lett 311: 199-211.

389 Faure F, Troiliard G, Nicollet C, Montel J-M (2003) A developmental model of olivine morphology as a  
390 function of the cooling rate and the degree of undercooling. Contrib Mineral Petrol 145: 251-263

391 Fleet ME, Bilcox GA, Barnett R L (1980) Oriented magnetite inclusions in pyroxenes from the  
392 Grenville province. Canad Mineral 18: 89-99

393  
394 Hart SR and Davis KE (1978) Nickel partitioning between olivine and silicate melt. Earth Planet Sci  
395 Lett 40: 203-219

396 Kamenetsky VS, Kamenetsky MB, Sobolev AB, Golovin A, Demouchy S, Faure K, Sharygin VV,  
Kuzmin

397 DV (2008) Olivine in the Udachnaya-east kimberlite (Yakutia, Russia): Types, compositions and 398  
origins. J Petrol 49: 823-839

399 Khisina, NR, Wirth R, Abart R, Rhede D, Heinrich W (2013) Oriented chromite–diopside symplectic  
400 inclusions in olivine from lunar regolith delivered by “Luna\_24” mission. Geochim. Cosmochim. Acta  
401 104: 84–98.

402  
403 Kreston P. (1973) The geology of Lemphane pipes and neighbouring intrusions. In: Nixon, PH (ed.).  
404 Lesotho Kimberlites, Cape and Transvaal Printers, pp159-167.

1  
2  
3  
4  
5  
6  
7  
8  
9  
11  
12 405 Kreston P, Dempster AN (1973) The geology of Pipe 200 and the Malibamatso dyke swarm. In: Nixon,  
13  
14 406 PH (ed.). Lesotho Kimberlites, Cape and Transvaal Printers, pp172-179.  
15  
16 407 Li C, Thakurta J, Ripley EM (2012) Low-Ca contents and kink-banded textures are not unique to  
17 18 408 mantle olivine: evidence from the Duke Island complex, Alaska. *Mineralogy and Petrology*  
104:147–19  
20 409 153.  
21  
22 410  
23 411 Lim E, Giuliani A, Phillips D, and Goemann K (2018) Origin of complex olivine zoning in olivine from  
24  
25 412 diverse, diamondiferous kimberlites and tectonic settings: Ekati (Canada), Alto Paranaiba (Brazil)  
and  
26 413 Kaalvallei (South Africa). *Mineralogy and Petrology* S112 suppl. 2: S549 – S554.  
27  
28  
29 414 Marsh JS, Hooper PR, Rehacek J, Duncan RA Duncan AR (1997) Stratigraphy and age of Karoo basalts  
30  
31 415 of Lesotho and implications for correlations within the Karoo igneous Province. *American*  
32 416 *Geophysical Union, Monograph 100, Large igneous provinces: continental, oceanic and planetary*  
33  
34 417 *flood basalts*, pp247-272  
35  
36  
37 418 Matzen AK, Baker BM, Beckett JR, Stolper EM (2013) The temperature and pressure dependence of  
38 419 nickel partitioning between olivine and silicate melt. *J Petrol* 54: 2521-2545  
39  
40  
41 420 Mitchell RH (1997) Kimberlites, orangeites lamproites, melilitites and minettes – a petrographic  
42  
43 421 atlas. Almaz Press, Thunder Bay, 243pp.  
44  
45  
46  
47  
48  
49  
50  
51  
52  
53  
54  
55  
56  
57  
58  
59  
60  
61  
62  
63  
64  
65



1  
2  
3  
4  
5  
6  
7  
8  
9  
45  
46  
47  
48  
49  
50  
51  
52  
53  
54  
427  
428  
429  
430  
431  
432  
433  
434  
435  
10  
11  
12  
13  
14  
15  
16  
17  
18  
19  
20  
21  
22  
55  
56  
57  
58  
59  
60  
61  
62  
63  
64  
65

422 Moore AE (1988) Olivine: a monitor of magma evolutionary paths in kimberlites and olivine  
423 melilitites. Contrib Mineral Petrol 99: 238-248.

424  
425 Moore AE (2012). The case for a cognate, polybaric origin for kimberlitic olivines. Lithos 128: 1-  
426 10.

427 Moore, AE (2017) Quantitative modelling of the apparent decoupling of Mg# and Ni in kimberlitic  
428 olivine margins: Comment on “Cordier et al., Metasomatism of the Lithospheric mantle...” (Journal  
429 of Petrology, 56, 1775-1796, 2015). J Petrol 58: 385-390

430  
431  
432 Moore AE Costin, G (2016) Kimberlitic olivines derived from the Cr-poor and Cr-rich megacryst  
433 suites. Lithos 258-259: 215-227

434 Moore AE, Erlank AJ (1979). Unusual olivine zoning: evidence for complex physico-chemical changes  
435 during the evolution of olivine melilitite and kimberlite magmas. Contrib Mineral Petrol 70: 391-405

436 Moss S, Russell JK, Scott-Smith BH, Brett R (2010) Olivine crystal size distribution in kimberlites. Am  
437 Mineral 95: 527-536

438 Nicolaysen LO, Ferguson J (1990) Cryptoexplosion structures, shock deformation and siderophile  
439 concentration related to explosive venting of fluids associated with alkaline ultramafic magmas.  
440 Tectonophysics 171: 303-335

441 Scott-Smith BH, Skinner, EMW, Loney PE (1989) The Kapamba lamproites of the Luangwa Valley,

1  
2  
3  
4  
5  
6  
7  
8  
9  
23 442 eastern Zambia. In: Ross, J. et al. (eds) Proceedings of the 4<sup>th</sup> International Kimberlite Conference,  
24  
25 443 vol. 1, Geological Society of Australia Special Publication 14: 189-205  
26  
27 444 Skinner EMW (1989) Contrasting Group I and Group II kimberlite petrology: towards a genetic model 28  
29 445 for kimberlites. In: Ross, J. et al. (eds) Proceedings of the 4<sup>th</sup> International Kimberlite Conference, vol.  
30  
31 446 è1, Geological Society of Australia Special Publication 14: 528-544  
32  
33 447 Smith CB, Sims K, Chimuka L, Duffin A, Beard AD, Townsend R. (2004). Kimberlite metasomatism at  
34  
35 448 Murowa and Sese pipes, Zimbabwe. Lithos 76: 219-232  
36  
37  
38 449 Sparks RSJ, Baker L, Brown RJ, Field M, Schumacher J, Stripp G, Walters A (2006) J Volcanol  
39 450 Geothermal Res 155: 18-48  
40  
41  
42 451 Welsch B, Faure F, Famin V, Baronnet A, Bachèlery P (2012) Dendritic crystallization: a single process  
43  
44 452 for all the textures of olivine in basalts. J Petrol 54: 539-574  
45  
46 453 Wilson, AH, (1982) The geology of the Great Dyke, Zimbabwe: the ultramafic rocks: Journal of  
47  
48 454 Petrology 23: 240–292  
49  
50 455 Yao Z, Qin K, Xue S (2017) Genetic relationship between deformation and low-Ca content in olivine  
51 52 456 from magmatic systems: evidence from the Poyi ultramafic intrusion, NW China Mineralogy and 54  
457 Petrology 111: 909–919  
53  
458  
459 Yudovskaya MA, Kinniard JA, Sobolev A., Kuzmin DV, McDONALS I, Wilson AH (2013) Petrogenesis  
of

1  
2  
3  
4  
5  
6  
7  
8  
9  
10  
11  
12  
13  
14  
15  
16  
17  
18  
19  
20  
21  
22  
23  
24  
25  
26  
27  
28  
29  
30  
31  
32  
33  
34  
35  
36  
37  
38  
55  
56  
57  
58  
59  
60  
61  
62  
63  
64  
65

460 the Lower Zone, olivine-rich cumulates beneath the Platreef and their correlation with the 461  
recognized occurrences in the Bushveld Complex. *Economic Geology*, 108: 1923-1952.

462 Yudovskaya M, McCreesh M, Costin G Kinnaird JA (2018) Spinel symplectites and associated reactive  
463 textures throughout the Bushveld magmatic section. Abstracts of the 13<sup>th</sup> International Platinum  
464 Symposium, 30 June -7 July 2019, Polokwane, South Africa.

465

466

467

468

469

470

471

472

473

474

475

1  
2  
3  
4  
5  
6  
7  
8  
9  
39  
40  
41  
42  
43  
44  
45  
46  
47  
48  
49  
50  
51  
52  
53  
54

476

477

478

479

480

481

482

483

484

485 **FIGURE CAPTIONS**

486 Fig. 1. Jointing in Karoo basalt parallel to the contact with the Lemphane blow (Northern Lesotho).  
487 Arrow marks the actual contact (From Kreston and Dempster, 1973, Plate 44b, and included with  
488 permission of Peter Kreston, 2018).

489

10

11 490 Fig. 2 Incipient shearing in the olivine-rich Rabele Dyke 166, Malibamatso Dyke swarm, northern  
12 Lesotho highlands. Note the partings (cleavages or fractures), sub-parallel to the incipient shear  
13 491 zones in some, though not all, of the olivine macrocrysts. (From Kreston and Demster, 1973, Plate  
14 492 15  
16 493 45B, included with permission of the first author.)

55  
56  
57  
58  
59  
60  
61  
62  
63  
64  
65

1  
2  
3  
4  
5  
6  
7  
8  
9  
17  
18  
19  
20  
21  
22  
23  
24  
25  
26  
27  
28  
29  
30  
31  
32  
33  
34  
35  
36  
37  
38  
39  
40  
41  
42  
43  
44  
45  
46  
47  
48  
49  
55  
56  
57  
58  
59  
60  
61  
62  
63  
64  
65

494

Fig 3a. Inferred fractures with a strong preferred orientation in olivines from a dyke in the Murowa kimberlite cluster, central Zimbabwe. Diameter of coin = 25 mm. Sample kindly provided by Dr. Frieder Reichardt.

498

Fig. 3b. Detail of the sample illustrated in Fig. 3a

499

Fig. 3c. Slickensides associated with chlorite development on a micro-fault cutting a section of core from the Tsodilo Resources BK16 kimberlite, Orapa Cluster, Central Botswana. Diameter of coin: 18mm.

502

Fig. 3d Brittle fractures in a core section from the Du Toitspan kimberlite, kindly provided by Petra Diamonds. Note disruption of two olivine macrocrysts by the left-hand vein. The fractures are calcite-filled, except where they disrupt the olivine macrocrysts, and contain serpentine. Diameter of coin: 20mm

506

507

Fig. 4a. Equant, euhedral olivine from the de Beers Kimberlite, Kimberley pipe cluster (PPL).

508

Fig. 4b illustrates the same olivine in XPL. Note the abundance of fluid inclusions in both the interior

1  
2  
3  
4  
5  
6  
7  
8  
9  
50  
52  
53  
54  
511  
512  
513  
514  
515  
516  
517  
518  
10  
11  
12  
13  
15  
16  
17  
18  
19  
20  
21  
22  
23  
24  
26  
27  
28  
29  
55  
56  
57  
58  
59  
60  
61  
62  
63  
64  
65

509 and margins of the crystal, the fractures, which traverse the olivine interior to margin, and the non51  
uniform extinction.

Fig. 4c. Euhedral olivine phenocryst (upper centre) from the de Beers Kimberlite (Kimberley cluster, South Africa) with the contrasting grey tone interference colours reflecting sharp compositional differences between core and rim (XPL). The shape of the core is slightly rounded, with minor embayments at the bottom. Note the equant shapes of the associated euhedral micro-phenocrysts, and fractures traversing grain interiors and margins of a majority of the olivines.

Fig. 4d. Euhedral olivine phenocryst from the WAT olivine melilitite, Namaqualand cluster, South Africa, with domains of contrasting extinction which traverse the core and rim of this crystal (XPL).

Fig. 4e. Hopper olivine in the Dikdoring olivine melilitite, Namaqualand, NW South Africa (PPL).

Fig. 4f (XPL) illustrates the domains of non-uniform extinction traversing core to rims of this olivine.

Fig. 4g . Olivines showing undulose extinction in dunite cumulate (UMT6-1449) from the northern limb of the BIC (from Yudovskaya et al., 2013).

Fig. 4h. Kink –banding in olivine from a harzburgite cumulate, northern limb of the BIC (image by M. Yudovskaya).

Fig. 5 (Data from Moore & Erlank, 1979). Olivines from the olivine melilitite designated BIES, from the farm Biesiesfontein, Namaqualand pipe cluster, north-western South Africa. Circles: olivine cores; squares: olivine rims. Diamond and star reflect a very subordinate population which show

1  
2  
3  
4  
5  
6  
7  
8  
9  
30  
31  
32  
33  
34  
35  
36  
37  
38  
39  
40  
41  
42  
43  
44  
45  
46  
47  
48  
49  
50  
51  
52  
53  
54

528 inverse core-to-margin zonation.

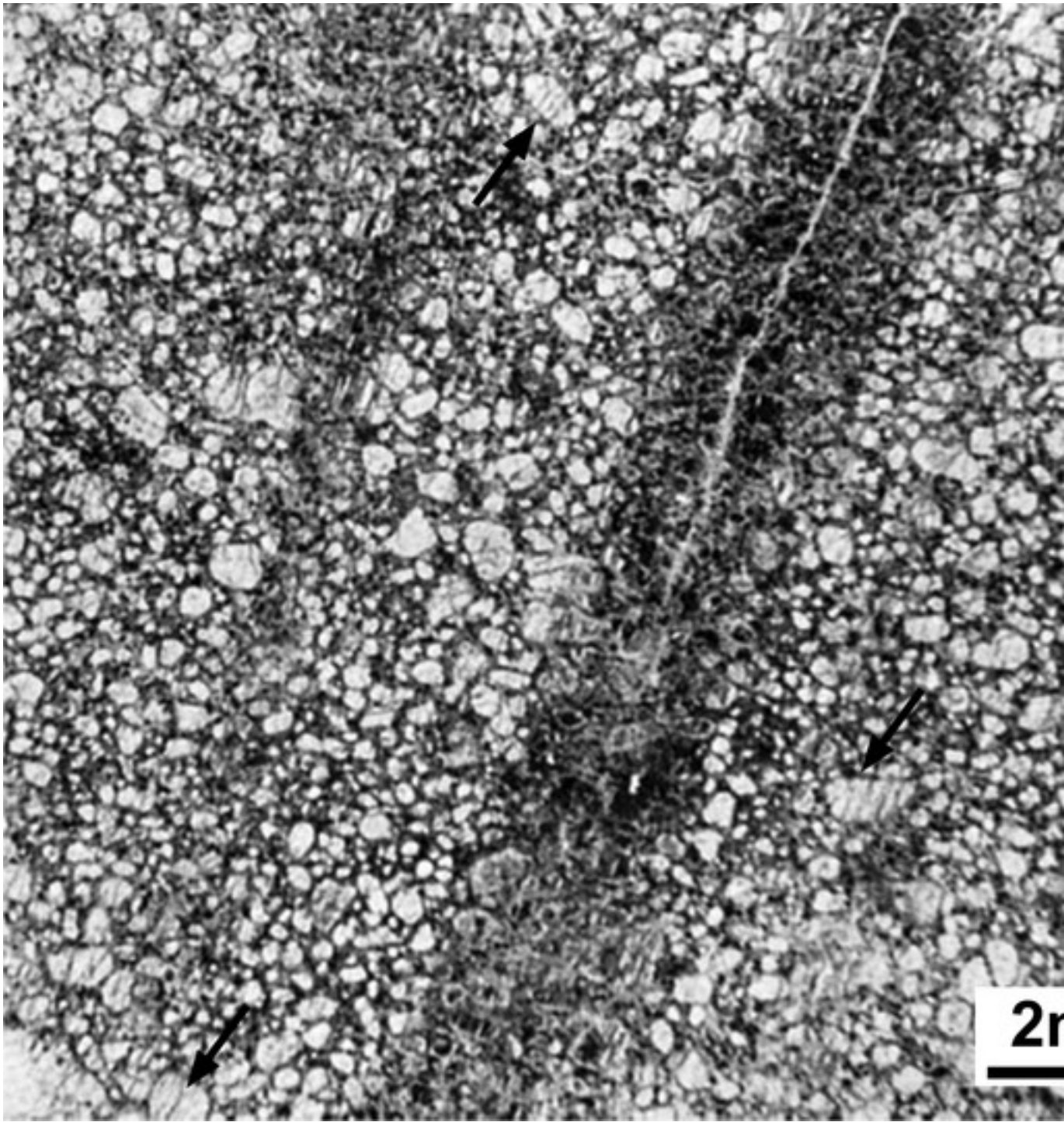
55  
56  
57  
58  
59  
60  
61  
62  
63  
64  
65

[Click here to access/download;Figure;Fig. 1-  
jointing.jp](#)





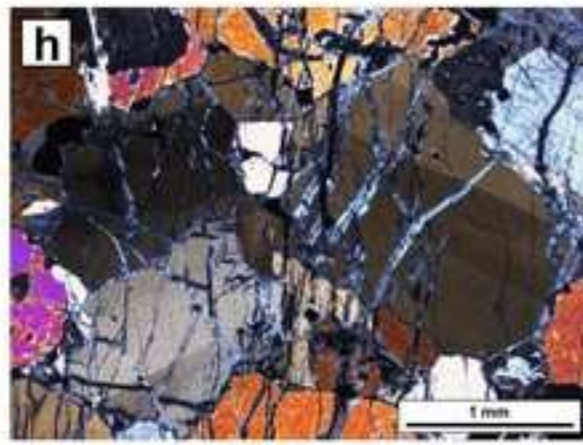
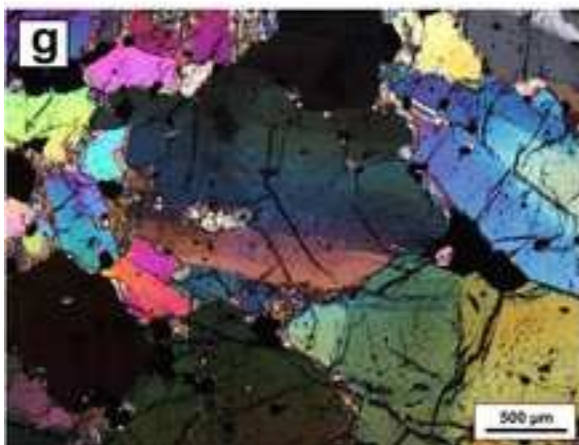
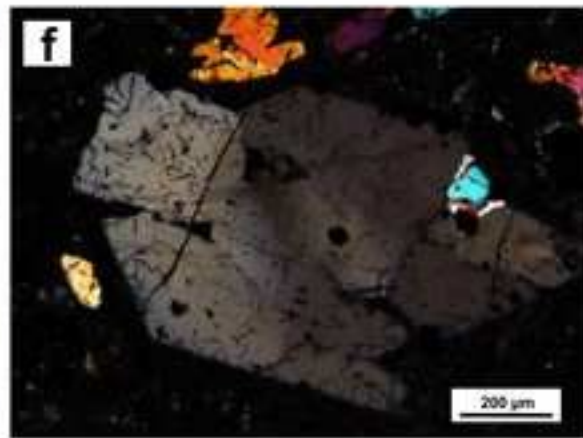
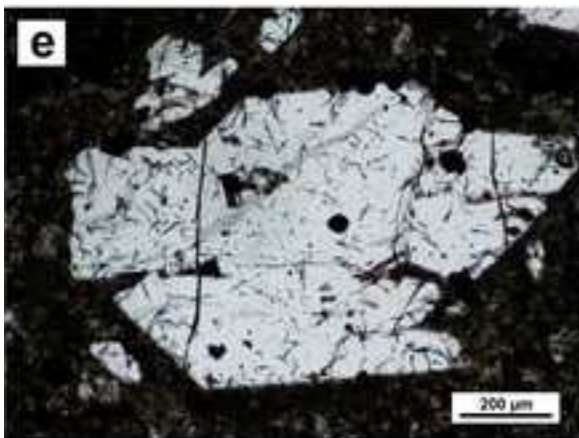
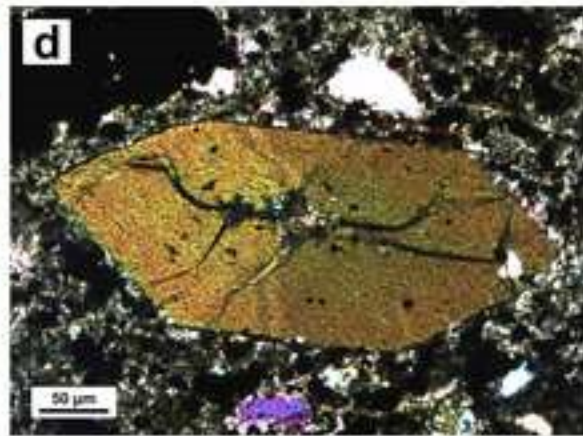
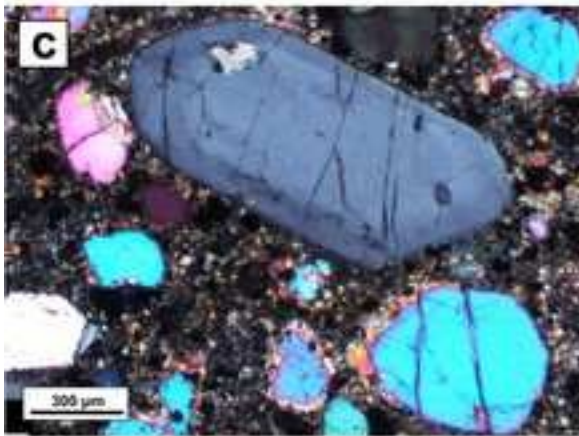
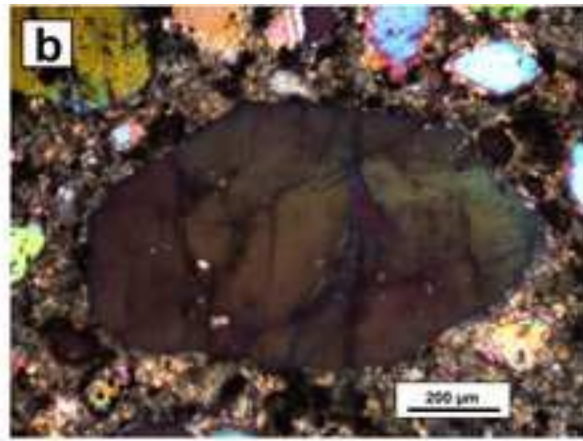
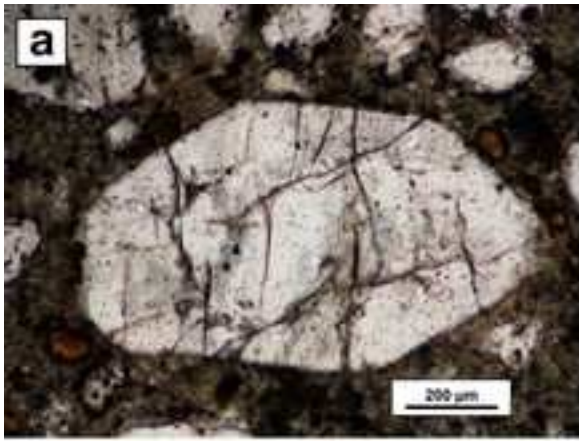
[Click here to access/download  
kimberlite.tif](#)



[Click here to access/download paper.jp](#)



[Click here to access/download;Figure;Fig. 4 Olivine paper.jpg](#)



[Click here to access/download](#)  
Olivines.jp

# BIES-3 Olivines

